

PSR B0809+74: Understanding its perplexing subpulse-separation (P_2) variations

Joanna M. Rankin^{1,*}, R. Ramachandran², and Svetlana A. Suleymanova^{3,4}

¹ Sterrenkundig Instituut “Anton Pannekoek”, 1098 SJ Amsterdam, The Netherlands
e-mail: jrankin@astro.uva.nl; joanna.rankin@uvm.edu

² Department of Astronomy, University of California, Berkeley, CA 94720, USA
e-mail: ramach@astron.berkeley.edu

³ Pushchino Radioastronomy Observatory of the Lebedev Physical Institute, 142290, Russia
e-mail: suleym@prao.psn.ru

⁴ Isaac Newton Institute of Chile, Pushchino Branch

Received 9 June 2004 / Accepted 28 August 2004

Abstract. The longitude separation between adjacent drifting subpulses, P_2 , is roughly constant for many pulsars. It was then perplexing when pulsar B0809+74 was found to exhibit substantial variations in this measure, both with wavelength and with longitude position within the pulse window. We analyze these variations between 40 and 1400 MHz, and we show that they stem primarily from the incoherent superposition of the two orthogonal modes of polarization.

Key words. stars: pulsars: general – polarisation – radiation mechanisms: non-thermal

1. Introduction

PSR B0809+74 surely remains one of the most studied and influential “drifters” in the pulsar literature. It exhibits all six of the fundamental pulsar phenomena: sub-pulse drifting, pulse nulling, profile mode switching, orthogonal emission modes, microstructure and “absorption”. Its well known ~ 11 -period fluctuation feature was identified by Taylor et al. (1969) only seven months after Drake & Craft’s (1968) discovery of the “drifting”-subpulse phenomenon (in B1919+21 and 2016+28), but their poor resolution prevented the feature from being prominent. Vitkevich & Shitov (1970) and Sutton et al. (1970) first exhibited the star’s marvelously precise “drifting” pulse sequences (hereafter PSs) early the next year, and the latter paper introduced the now standard terminology of P_1 , P_2 and P_3 for the pulsar rotation period, the subpulse-separation interval, and the driftband-separation period, respectively. Properties of these drifting subpulses have been investigated by many authors over the past three decades (e.g., Cole 1970; Taylor & Huguenin 1971; Backer et al. 1975). Its polarization properties have also been studied in detail by various investigators (Ramachandran et al. 2002; von Hoensbroech & Xilouris 1997; Gould & Lyne 1998).

A spectacular reported property of B0809+74’s subpulse drift is the apparent variations of mean separation of subpulses (P_2) with longitude and frequency. Different (and often

conflictual) values can be found in at least a dozen papers, and the reported frequency dependences, first in Taylor et al. (1975) and then in Bartel (1981) have influenced understanding of the properties of this pulsar greatly. According to Bartel (1981), the frequency dependence of P_2 is the same as that of the pulse width at various frequencies. He derives a frequency dependence of $P_2 \propto \nu^{-0.23}$. Similarly, its longitude-dependent variations have also been studied in the literature. According to van Leeuwen et al. (2002), the drift bands seen in this pulsar at 328 MHz are not “straight”, which implies that P_2 varies across the pulse profile. These circumstances pose a serious problem for the geometrical interpretation of drifting subpulses. If one assumes that these drifting subpulses are a set of subbeams in the magnetosphere of a pulsar and that they drift around due possibly to $\mathbf{E} \times \mathbf{B}$ forces, then it is very difficult to reconcile these observed longitude and frequency variations in subpulse spacing P_2 with such a geometrical standpoint.

Curiously enough, there appears to be little or no difficulty in defining P_2 at low frequency. Between 81.5 and 151 MHz, six writers give values around 53 ± 2 ms, or some 15.3° of pulse longitude (Cole 1970; Sutton et al. 1970; Vitkevich & Shitov 1970; Page 1973; Bartel et al. 1981; Davies et al. 1984). A key to understanding why this is so may follow simply from Davies et al.’s discussion: They find that the driftbands at 102 MHz are “essentially straight”, whereas those at 406 and 1412 MHz become increasingly curved. Our own more recent observations confirm this conclusion as can be seen in the 112.7-MHz PRAO observation in Fig. 1 (left). Many of the reported P_2 values at

* On leave from Physics Dept., University of Vermont, Burlington, VT 05405 USA.

around 400 MHz are only a little smaller than those above, apparently reflecting the fact that the driftbands curve in such a way as to parallel the low frequency behavior on the trailing edge of the profile. This can be very clearly seen in Davies et al.'s Fig. 4¹.

Only at 21 cm does the literature report very different behaviors (e.g., 29 ms, Bartel et al. 1981; 31 ms, Davies et al. 1984), and the reason for this can first be discerned in Wolszczan et al.'s (1981) Fig. 5a. Here we see that the drift-modulation phase exhibits a discontinuity near the profile peak amounting to about $+180^\circ$ – a circumstance which Edwards & Stappers (2003; hereafter E&S) as well as ourselves (see Fig. 4), have also confirmed. Clearly, most early P_2 determinations at 21 cm were carried out in the vicinity of this drift-phase discontinuity under low signal-to-noise conditions in which this phase “jump” was not resolved, thus it is not at all surprising that very different values were obtained. Wolszczan et al. obtain much larger P_2 values, and if the 180° “jump” is roughly corrected for – that is, by estimating that 1.5 modulation cycles occur over about a 20° longitude interval in their Fig. 5a – we find that P_2 over the entire width of the profile may well be not far from the quoted 47 ms or 13.1° . This value, in turn, compares well with the 100-MHz value of 15.3° , being only a little smaller (owing to the reduced overall scale of the profile) as might be expected – a conclusion also reached by Edwards & Stappers (2003) who argue that the modulation-phase rate must be independent of frequency.

The origin, however, of the phase jump remains as yet unexplained. Why, perversely, should the phase rate – which is nearly linear at low frequency – first steepen in the centre of the profile at meter wavelengths and finally exhibit a 180° discontinuity at 21 cm? The reason, almost certainly, is modal polarization which we will try to demonstrate concretely below. We must also stress that virtually every existing drift-modulation study of pulsar B0809+74, historical and more recent, was based entirely on the total power (Stokes I). We will return to this argument once we have first both discussed our observations and what is known of the star's modal polarization.

2. Observations

Observations used in our analyses below come from several different sources. We make considerable further use below of the same remarkably bright, 328-MHz polarized pulse sequence acquired using the Westerbork Synthesis Radio Telescope (hereafter WSRT) on 2000 November 26 and first studied by Ramachandran et al. (2002). This observation has now been corrected for a recently determined instrumental effect that converted some linear into circular polarization (Edwards & Stappers 2004; see their Appendix). The 1.38-GHz observation was also made using the WSRT on 10 January 2002 using an 80-MHz bandwidth, a 0.8192-ms sampling interval, and 256 effective channels across the passband.

¹ The 40.9-MHz phase rate in Fig. 1b implies a substantially larger P_2 value, some 65 ms or 18° , apparently reflecting the overall larger longitude scale of the profile at this low frequency. We will discuss the implications of this value in a subsequent paper.

The 112.7-MHz observations were made at the Pushchino Radio Astronomy Observatory (PRAO) using the BSA (Bolshaya Synfavnaya Antenna) telescope at 112.7 MHz². The signals from the linearly polarised array were fed to a radiometer with 128×20 -kHz contiguous channels in order to measure the total intensity and its spectral variations across the passband. The dedispersed pulses were referred to the frequency of the first channel – that is, to 112.67 MHz. By observing a partially linearly polarised pulsar signal at adjacent frequencies the rotation measure can be obtained, and this in turn used to determine the linear polarization (Suleymanova et al. 1988) from the Faraday-rotation-induced, quasi-sinusoidal intensity modulation across the passband. The time resolutions were 2.56 ms or 0.71° . The observations were comprised of 555 pulse periods as limited by the BSA's beam. The remarkable 41-MHz observation was acquired with PRAO's DKR-1000 instrument, using a 128×1.25 -kHz radiometer and 5.12-ms integration. The 27 December 2003 recording includes a nearly interference-free segment 947 pulses long, which was used for the present analysis. Our analyses are based on high quality pulse sequences from which the null intervals have been removed, as indicated by the analyses and techniques developed by van Leeuwen et al. (2002). Such a removal represents a first-order correction to the well known subpulse-phase near stasis across nulls. The effects cannot be completely removed, however, both because of higher-order effects and because some number of nulls, less than one P_1 in duration, will occur when the star beams in other directions.

3. Properties of orthogonal modes in PSR B0809+74

A very important property of pulsar subpulses is that they do not have any memory of their polarization state. During their drift though our sightline, as we see in all pulsars that exhibit drifting-subpulse behaviour, their polarization state changes continuously and appears to depend entirely on their location within the “pulse window” or profile. This can be seen very clearly for pulsar B0809+74 at 328 MHz in the colour display given by Ramachandran et al. (2002) as their Fig. 4, where the two polarization modes have about equal strength, but vary dramatically – and very systematically – in relative intensity throughout the profile³. The behaviour is also demonstrated, using mode-segregation methods, for B0809+74 as well as other bright pulsars (see Fig. 3 of Rankin & Ramachandran 2003).

Figure 2 provides an average, but accurate means of assessing the polarization characteristics of the “drifting”-subpulse pattern. Its six panels give partial profiles corresponding to successively increasing intervals of phase within the star's overall ~ 11 - P_1 modulation cycle. We thus see in a “cyclical”

² The instruments are fully described in the Pushchino Observatory website: <http://www.prao.psn.ru>

³ The circular polarization in this display should be discounted, and the fractional linear taken as being about 50% greater per the recent WSRT recalibration by Edwards & Stappers (2004). The configurations of modal polarization, however, remain nearly unaltered.

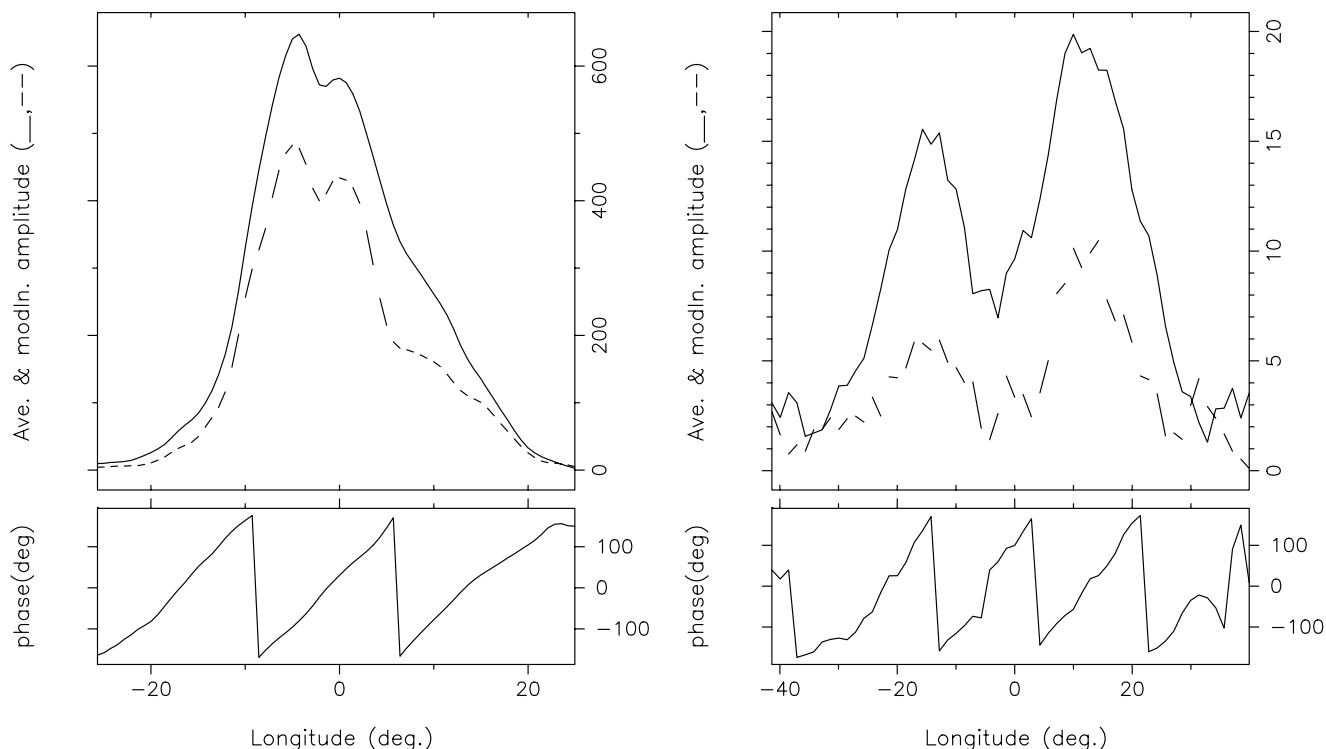


Fig. 1. The total-power modulation amplitude and phase of B0809+74 at 112.7-MHz (left) and 40.9 MHz (right). The Stokes I profile (solid) and modulation amplitude (dashed) are given in the upper panel; whereas the modulation phase is plotted in the lower panel. Note that here the phase rate is essentially constant over the body of the profile (except, as expected, in the very center of the 40.9-MHz profile), unlike that at higher frequencies. These PRAO observations were recorded on 2 December 2000 and 27 December 2003, respectively.

(*abcfed/a*) order polarized subpulses appear on the trailing edge of the total-power profile (at longitudes near 20°) and then drift progressively toward earlier longitudes from panel to panel. The sensitivity of the analysis is such that the average subpulse position and properties can be traced through nearly three rotations around the plots, representing an interval in longitude of thrice the subpulse spacing – or, what is the same, that we generally see three subpulses in each plot (or individual pulse), with one barely appearing on the extreme trailing edge of panel *a* and another close to disappearing on the extreme leading edge in panel *f* or even *e*⁴.

A remarkable aspect of these subpulses is that they are so obviously polarized in a modal manner. Subpulses appearing to the left of the diagrams are substantially linearly polarized and have negative PA values; whereas, subpulses that are waning at the right of the diagrams also have a fairly large linear polarization with positive PA values. (Here the modal PA tracks fall conveniently about the PA origin in a roughly symmetrical manner; their individual behavior is very clear, for instance, in panel *b*). What is arresting, however, is the behavior in between these extremes: the (average) subpulses peaking in the range between about 10 and 4° longitude are both depolarized and show a sharp modal transition – and note that the modal depolarization and PA “jump” marking this transition moves in

an orderly manner from the trailing edge of the following subpulse in panel *e*, to the center of the bright subpulse in *d*, and then to its leading edge in panels *a* and *b*.

The displays of Fig. 2 compliment what we can see in Ramachandran et al.’s Fig. 4. There, the driftbands can be traced in total power (Stokes I) over almost as great a longitude interval, but the polarization can be delineated only over a span somewhat greater than P_2 . However, in the region near the 328-MHz profile peak, the colour pulse-sequence (hereafter PS) display provides better resolution of the polarization changes. (Note that the longitude scale of this PS display is not the same as that of Fig. 2.) Also, note that the fractional linear polarization and angle are remarkably consistent over the entire 200 PS displayed; whether one mode or the other is active (red vs. green coded angles in the 3rd column) L/I is about 60% (with the 50% calibration enhancement mentioned above). Finally, note that the modal “tracks” in positive (green-cyan) PAs are not parallel to those in total power; these have a somewhat larger apparent “driftrate” and are encountered at earlier longitudes; whereas the other mode (red-magenta PAs) is encountered later and is more parallel to the total-power drift “track”. Indeed, the overall effect of the latter is to broaden the driftband at and before the average profile peak.

While these effects can only be estimated when looking at the polarized PS display, Fig. 2 exhibits their effect more clearly. The (average) subpulses near the peak of the profile exhibit adjacent regions of modal power and are thereby somewhat broader in width. This is close to what Davies et al. (1984)

⁴ Manchester et al.’s (1975) Fig. 7 also clearly shows this progress of modal polarization effects along the driftband, but not in a form where the relationships between adjacent subpulses can be accurately discerned.

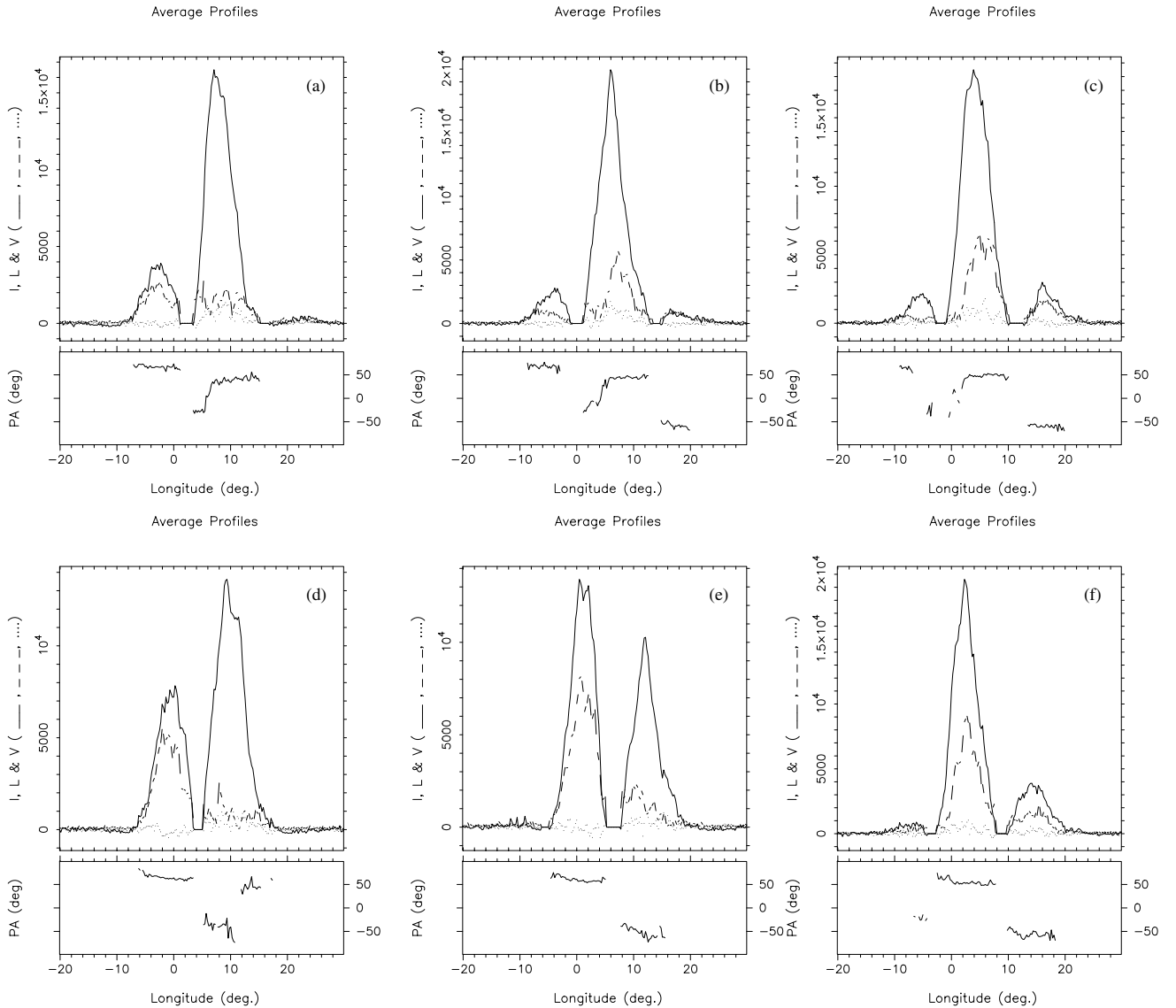


Fig. 2. “Cyclical” clockwise composite of 6 partial polarisation profiles (*abcfed/a, ...*) folded at 60° phase intervals around the nominal $11-P_1$ modulation cycle at 328 MHz. All were computed from the same section of this (recalibrated) observation, and two or three subpulses are seen which “drift” steadily from later to earlier phases about $1-2^\circ$ from plot to plot. The outside curves give the total power (Stokes parameter) I , the dashed ones the linear polarization L ($=\sqrt{Q^2 + U^2}$), the dotted ones the negligible circular polarization V , and the others the polarization angle χ ($=0.5 \tan^{-1} U/Q$). Note that the earliest subpulses (here folded to an average) have a positive PA, while the latest have a negative PA. The broader central subpulses exhibit the most interesting behavior, often showing adjacent regions of modal polarization and substantial depolarization. Panels *e* clockwise around *b* exhibit this behavior very clearly. Note the depolarization in the first two as well as the PA “jumps” in the last three. Can it be doubted that modal polarization effects play a major role in the pulsar’s strange longitude variations in subpulse width and spacing P_2 ?

observed at their nearby frequency of 406 MHz as seen in their Fig. 5 (though a different behavior was observed at 102 MHz, which we will discuss below). A number of different geometrical and other effects contribute to the varying subpulse width and spacing as a function of longitude, but we cannot doubt that these systematic modal polarization transitions are a major contributor.

The orthogonal modes in B0809+74 also seem to have a different behaviour at different radio frequencies. For instance, at 112.7 MHz, the polarized emission is often more or less completely dominated by one of the modes across the full width

of the profile, as shown in Fig. 3. However, this is not the case at higher frequencies. At 328 MHz (see Figs. 2 and 1 of Ramachandran et al. 2002⁵), both the modes are clearly present, although with varying strengths across the profile. In fact, for a limited longitude range around the peak of the average pulse, strong subpulses dominated by both modes occur. However, one mode dominates most subpulses in the leading part of the profile, and the other mode dominates in the trailing

⁵ Note that we now know that the linear power is about 50% greater than as shown in this figure because of the recalibration mentioned above.

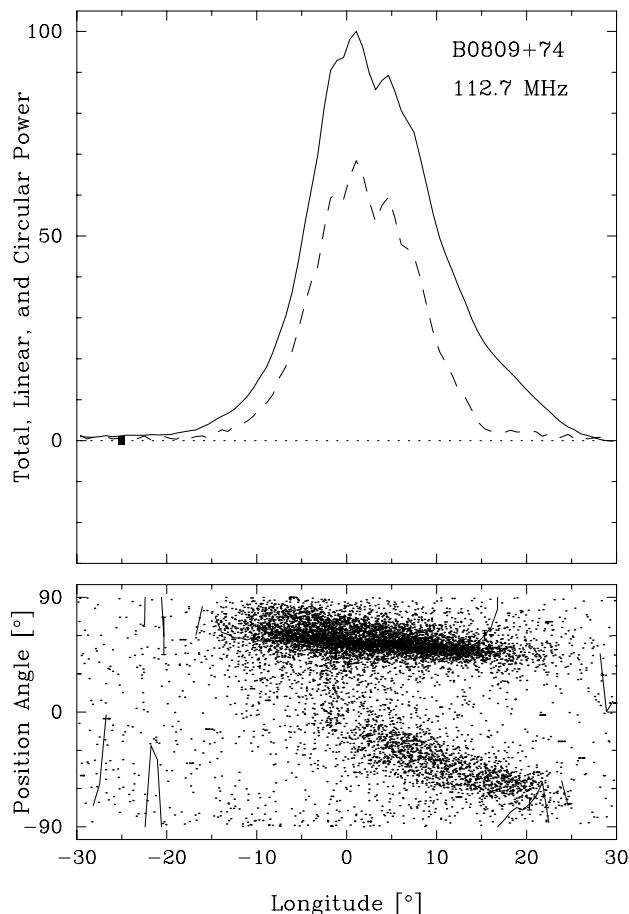


Fig. 3. Polarization histogram of a 112.7-MHz PRAO observation of 6 February 2000. The solid and the “dashed” lines give total power and linearly polarized average profiles. A high degree of linear polarization is often seen at this frequency, wherein one polarization mode seems to dominate. The linear polarization PA is given in the bottom panel as a function of pulse longitude. The longitude reference here is arbitrary, and the circular polarization was not measured so the dotted curve falls at zero.

part. The orthogonal PA “jump” in the average profile occurs somewhere around the peak of the profile, but the low linear polarization throughout the profile shows that modal depolarization is a factor everywhere. This sort of behavior is seen clearly in the early polarimetry of Lyne et al. (1971) as well as in the 234- and 606-MHz profiles of Gould & Lyne (1998)⁶.

At higher frequencies, a different and quite unusual phenomenon appears, where the leading edge of the profile becomes almost fully linearly polarized. This can be seen at and above 925 MHz in Gould & Lyne and is very finely exhibited in the 1.41- and 1.71-GHz polarimetry of von Hoensbroech & Xilouris (1997). Nearly complete linear polarization is virtually unknown among conal single (S_4) stars, and remarkably suggests (a) that only one polarization mode is observed in this longitude range; and (b) that it is almost fully linearly polarized! Once, then, we have gazed on this splendid 1.41-GHz profile, in

which the entire uni-modal leading edge up to the 75% power point is fully polarized and then noted the precipitous falloff in linear polarization to virtual depolarization on the trailing edge – a region where the two modes must be active with a depolarizing effect – can we doubt that there will be a phase boundary of some sort between these two contrasting modal behaviors? – And, this phase boundary falls precisely where it must: between the peak and the trailing 3-dB point of the linear power – or just before the PA excursions in the above profiles.

4. PSR B0809+74’s P_2 variations

Careful perusal of our Fig. 2 above demonstrates that P_2 must vary as the modal configuration of the mean subpulses varies with longitude across the profile. A steepening will then certainly occur near the center of the total intensity profile where fully double-modal subpulses must be fitted (crowded) into the driftbands. Apparently, the somewhat simpler situation at low frequency arises because one mode dominates across most of the profile, so that their joint effect changes little with longitude. That this is so can be seen in the 112.7-MHz polarization histogram shown in Fig. 3; note both the large fractional linear polarization and dominance of a single polarization mode across most of the profile.

We have, however, not yet directly demonstrated in any detail that B0809+74’s P_2 anomalies are due to modal polarization effects. Surely, we should expect that virtually any sightline traverse along the edge of a conal beam will encounter systems of modal “beamlets”, and we have shown (Ramachandran et al.’s (2002) Fig. 4) that the observed “beamlet” structure varies with longitude across the profile, but it remains to see what specific modal effects are responsible for the historical difficulties that many investigators have had in determining the star’s P_2 , especially at around 1400 MHz.

First, let us examine in our own observations what others may have seen at 1.4 GHz. Figure 4 gives a total-power average profile for the pulsar at 1380 MHz and shows how the modulation phase varies across it. The modulation-feature width here is several FFT bins wide, so that only about 10% of the power falls at the fluctuation frequency in question. Here, however, we see the usual phase rate – corresponding to a P_2 of about 13° – under the trailing half of the profile (and the adjacent frequency bins behave similarly). Note that the phase rate on the extreme leading edge of the profile is near this value, but that it steepens rapidly and then exhibits a large discontinuity near the longitude origin. This behavior is very similar to that first reported by Wolszcan et al. (1981: Fig. 5a) and more recently by Edwards & Stappers (2003: Fig. 2b), but it is very unlike anything we have thus far encountered at lower frequencies.

In order to explore the polarization structure of the “drift”-modulation, we have computed IQV Stokes sequences in which nearly all of the linearly polarized power is rotated into a single Stokes parameter Q' . To the extent that the polarization modes are orthogonal, they can be represented simply in terms of positive or negative contributions to Q' – and if U' is then found to contain only a negligible level of noise-like power, this procedure is well justified. Q' then has the character of V in representing the linearly polarized power along a principal axis

⁶ The Gould & Lyne (1998) 410-MHz profile seems exceptional in this regard. Perhaps the star exhibits some modal variability, but both our own observations as well as those of Manchester (1971) around this frequency confirm the above behaviour.

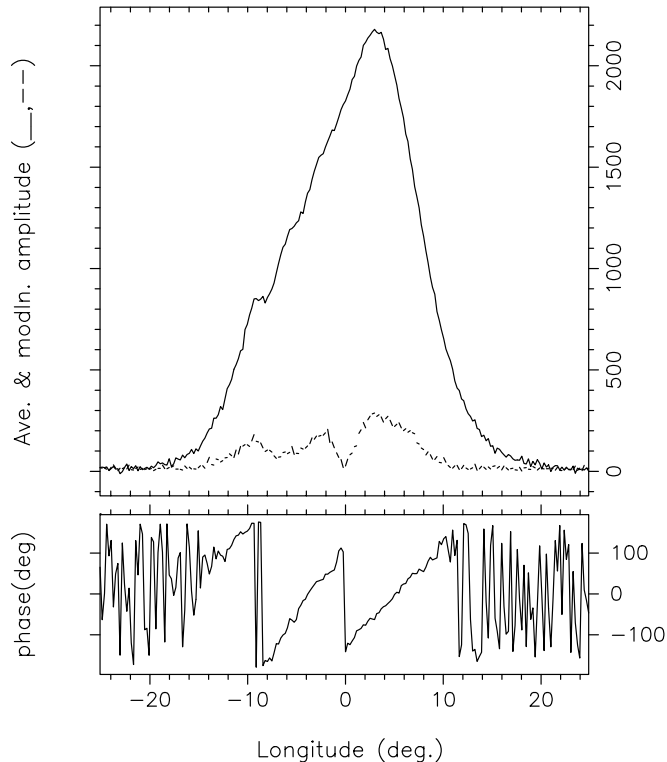


Fig. 4. Average profile (solid line), modulation amplitude (dotted line) and modulation phase (bottom panel) at 1.38 GHz. The phase rate here varies a good deal across the profile and exhibits the discontinuity near the longitude origin first resolved by Wolszcan et al. (1981). Note, however, that the phase rate on the leading and trailing edges of the profile is not far different than that seen at the lower frequencies. This WSRT observation was recorded on 10 January 2002.

of the Poincaré sphere – and given that this power is modal, the two modes will have opposite signs.

We have computed this $IQ'V$ sequence for our WSRT observations at 328 and 1380 MHz. In both cases the nulls had already been identified and removed, so that large portions of each null-removed sequence exhibited a very high- Q modulation feature. We tested the efficacy of this procedure by examining the Stokes- U' PSs, and in both cases we found that so little modulation power remained in them that no fluctuation feature corresponding to the usual $P_3 = 11P_1$ could be discerned. Virtually all of the modal fluctuation power was then represented by Q' .

Figure 5 shows the result of folding Q' over the precisely determined $11-P_1$ modulation cycle at 328 MHz. The colored driftbands represent the behavior of the polarized modal power. It is immediately clear from the main panel that this power is not at all symmetrically distributed, as the positive (yellow-red) driftband spacing (i.e., P_2) is markedly narrower than that of the negative (blue-green) mode. Also we can see that if integrated along each driftband, the negative mode exhibits a fairly flat power profile, while that of the positive mode is peaked and slightly skewed to the left. These are then the linear polarization characteristics which greatly complicate the P_2 determination in total power. One might measure a fairly consistent (but distinct) value of P_2 for each polarization mode across the

entire pulse profile at 328 MHz; however, when only the intensity of these modal contributions is measured, there is no way to discern how complex and non-linear is their joint effect. Note, for instance, how the Q' power varies over the modulation cycle in the left-hand panel and how it is distributed in longitude in the lower one.

Using this same method, we can approach the questions which prompted this discussion: (i) why is P_2 so difficult to determine at 1.4 GHz; and (ii) what causes the modulation-phase “jump” near the center of the profile? Both Figs. 6 and 5 are produced by folding the respective time sequence precisely at P_3 . Notice how differently the modal polarization power behaves at 1380 MHz when compared with 328 MHz in the previous figure. True, the leading edge of the profile is modulated by one bright mode, and the other appears more active within the later part of the profile. We can see clearly in the bottom panel that the two modes have about equal intensity (Q' about zero) at positive longitudes – and this in strong contrast to the early part of the profile.

We saw at 328 MHz that the driftband phase cannot be linear across the profile, because subpulses with both polarization modes must be accommodated in an environment where the drift involves only a single mode on the profile wings. Here, at 1.38 GHz we see a very different behaviour: subpulses in the leading half of the profile exhibit only a single polarization mode, whereas those in the trailing half reflect about equal contributions of both modes. At the lower frequency, the two modes lie immediately adjacent to each other along modal subbeam “tracks” only a few degrees wide, apparently assuming their positions along the driftband with such a precision that a line of modal depolarization is hardly discernible in Fig. 5. Indeed, this is just what we see in the PS polarization display in Ramachandran et al.’s (2002) Fig. 4.

At 1.4 GHz, however, we see a very conspicuous region near the centers of both the profile and the driftband, where the driftband appears to cease and then restart. This represents quite a different behaviour than just seen at lower frequency, where the modal driftbands parallel each other for a large portion of the modulation cycle. Here there seems to be some modal depolarization *along* the overall driftband, as might happen, for instance, if there is some longitude irregularity in the modal subbeam longitude positions. Indeed, the width of the driftband at 1.38 GHz does appear to be somewhat larger than that at 328 MHz, particularly under the first half of the profile.

In this rather complex context, we can well be less surprised that multiple experts have, over the years, found this pulsar’s P_2 so difficult to measure around 21 cm. Upon looking at Fig. 6 in more detail, though, we see that while the prominent modal driftbands on the leading and trailing edges of the profile have a drift rate that is compatible with that seen at lower frequencies, the modal driftband spacing in longitude is far less, about 9° , which indeed is one of the values often reported for P_2 at 1.4 GHz. Here we can see the consequences of this modal complexity fairly clearly, but when studied in total power, as has heretofore uniformly been the case, such artefacts of the polarization-modal modulation remain impossible to discern and decipher.

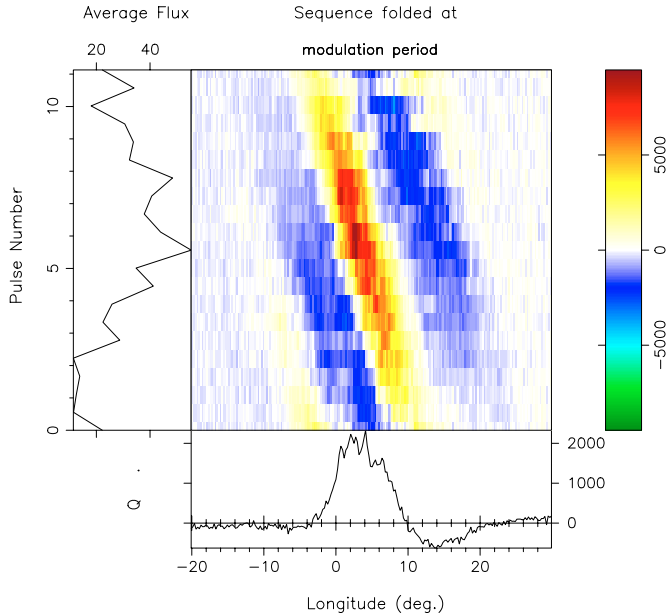


Fig. 5. Color intensity-coded diagram showing the distribution of linearly polarized fluctuation power as a function of longitude over the $11P_1$ modulation cycle at 328 MHz. One polarization mode is positive (yellow-orange-red) and the other negative (blue-cyan-green) in this representation. Note that the average Q' power (left-hand side panel) is quite small, reflecting the nearly complete linear depolarization at this frequency; whereas, the bottom panel shows that one mode (that here seen as positive) dominates in the early part of the profile and the other the later. See text for details.

Similarly, we can see here that the drift phase must change in the center of the profile at 1.4 GHz for almost exactly the same reason as the sign of Stokes parameter Q' changes. The initial part of this drift-phase trajectory is seen near the center of the diagram, where leftward-drifting subpulses develop comparable amounts of leading negative and trailing positive modal polarization. A drift-phase discontinuity must then occur just where the negative part of these symmetrically modally polarized subpulses ceases – that is, just where the positive mode suddenly becomes dominant in the lower panel. Most significantly, however, Fig. 6 shows us that the predominantly negative driftband trajectory established in the latter part of the profile first broadens, wanes and is then picked up again, almost at the same driftband phase, by the opposite polarization mode.

Or, said differently, Fig. 6 shows us that while the negative (blue-cyan-green) modal driftband in the latter part of the profile appears to extrapolate linearly to the positive (yellow-orange-red) one that continues in the earlier part of the profile, subpulses that are observed in total power will exhibit a modulation-phase “jump” at the modal boundary. This “jump” simply reflects the circumstance that the subpulses drifting into the middle of the profile from the trailing edge are polarimetrically bi-modal, whereas those in the earlier part of the profile exhibit only one mode. A modulation-phase step is then required across this modal drift discontinuity at about 0° longitude. Some non-linearity or discontinuity must “mark the spot”. Indeed, such a “jump” can only occur because increasingly

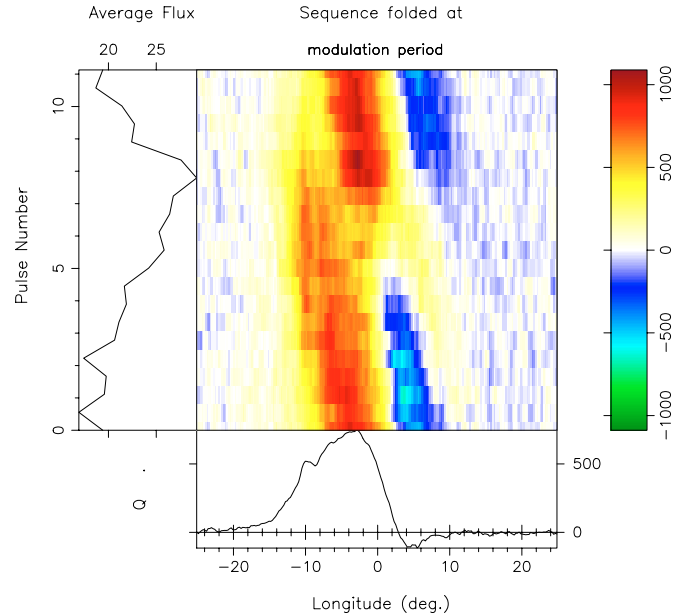


Fig. 6. Color intensity-coded diagram showing Q' at 1.38 GHz folded over the $11P_1$ modulation cycle as in Fig. 5. Notice that here the profile polarization is slightly positive (red-orange-yellow) over the entire modulation cycle (*left-hand panel*) but that this dominance is complete only during the leading part of the profile (see *bottom panel*). In the main panel we see that the subpulse modulation under the first part of the profile is produced entirely by the “positive” mode. The negative mode only appears after the longitude origin at just the point where Q' decreases sharply. There is indeed a good deal of the negative-mode (blue-cyan-green) fluctuation power here as well, and this results in the nearly zero aggregate linear power. The longitude interval between the bright red and blue-cyan bands is only some 9° , which is just what would be measured in the total power. However, the phase rate of each band is compatible with a P_2 of some 13° on the profile edges where it is dominant, as we have seen above. What this diagram shows most remarkably, however, is the way that the negative driftband ends surrounded by positive drift power and is then continued, almost precisely in line, by the positive drift band.

depolarized but orderly subpulses, on average (near the boundary), carry the phase up to the point of the “jump” on both sides. Probably, this means that subpulses associated with both the bi- and uni-polarization-modal driftbands occupy the “jump” region in successive pulses, giving rise to the reports of “confused” “drifting” in this central region.

This is a remarkable result. We thus now understand in an analytical sense how it is that the large phase “jumps” occur in the 21-cm total-power driftbands of B0809+74 – and perhaps some other stars as well. Edwards & Stappers (2003) have argued the such modulation-phase discontinuities can be produced by the superposition of out-of-phase modulation patterns, and here we see that such patterns can be generated by modal polarization. Note that the modal power patterns, integrated over the modulation cycle (bottom panels of Figs. 5 and 6) are not very different qualitatively; it is the dynamics of the modal power patterns which matter here. We still have much to learn, however, about what modal “beamlet” configurations and/or sightline geometries can give rise to such a counter-intuitive modulation-folded polarization pattern. This

result does demonstrate for us that, modal polarization effects apart, we can still think of the subbeams as passing our sightline with a relatively constant and basically geometrically-determined value of P_2 – or, what is the same, our fundamental cartoon conception of the subbeam configuration as a “carousel” survives. On this basis we can proceed much more confidently in our further attempts to determine the full subbeam configuration and circulation time of this complex star.

5. Summary and discussion

We have attempted in this paper to understand the character and causes of the (in)famous variations of subpulse spacing (P_2) in pulsar B0809+74. Some dozen published studies report both that the subpulse spacing changes measurably with longitude at a given frequency and that significantly different values are obtained at different frequencies. While this puzzling issue has lain dormant for several decades, it is essential to fully and accurately characterize the situation. B0809+74 is usually quoted as exemplifying such effects, and recent studies are beginning to identify less dramatic but still important such variations in other pulsars. If, in fact, we are to take the reported P_2 variations in B0809+74 as literally true, then it is very difficult to understand how the usual rotating-subbeam “carousel” interpretation of subpulse drift could be retained.

We find that B0809+74’s P_2 variations are primarily artefacts of modal polarization in total-power analyses. This is one of the many effects introduced by mixing of the quasi-orthogonal modes. We thus clearly demonstrate that the use of total-power PSs for pulse-modulation studies will often lead to confusing results due to polarization-mode mixing, just as they are well known to do when averaged to produce polarized profiles. Specifically, we find that

- The near constancy of P_2 at around 100 MHz and below is due to the circumstance that one polarization mode is often dominant. This results in the “straight driftbands” observed by earlier workers.
- Significant curvature is seen in the pulsar’s driftbands at 328 MHz, and this can be traced to the overlapping of the polarization modes over nearly the full width of the profile. The “straighter” driftbands on the leading and trailing edges of the profile occur in regions where one mode is dominant. Conversely, the most curved section of the driftband is found near the longitude of the profile peak where both modes are “crowded” into the same longitude interval at comparable intensities – and, of course, this is just where we find the profile most depolarized.
- At 21 cms nearly complete linear polarization is observed in the leading half of the profile – this in strong contrast to most other conal single stars which exhibit highly depolarized profiles. This suggests (a) that this polarization mode is fully linearly polarized (as the complete linear polarization rules out any contribution from the second mode); and (b) leaves a deafening question regarding the fate of the second mode.
- The trailing half of the pulsar’s 21-cm profile exhibits a nearly equal contribution from the two polarization modes

and is also very nearly depolarized. The boundary between the highly polarized leading region and the negligibly polarized trailing region – shown near 0° longitude in Figs. 4 and 6 – is precisely where the modulation-phase discontinuity is observed, arguing that the polarization and phase “jumps” are connected.

- The modulation-phase “jump” occurs in total-power analyses because the linear driftbands comprised of bi-polarization-mode subpulses cannot connect smoothly with those comprised of a single polarization mode.

In summary, studies of *drifting* subpulses necessarily entail sightline cuts along the outside edges of conal beams, precisely the region now known to present the most complex (and interesting!) polarization-modal effects (e.g., Rankin & Ramachandran 2003). If then modal polarization effects are the major cause of P_2 variations, it follows that modal effects must always be considered in measuring this fundamental parameter.

Acknowledgements. We thank Russell Edwards and Ben Stappers for interesting and useful discussions and their assistance with some of the Westerbork observations – and in particular their generously making available to us the results of their recent polarimetry calibrations. We also thank Joeri van Leeuwen for assistance with some of the observations, Avinash Deshpande for advice and use of his software, and Geoffrey Wright for discussions. Portions of this work were carried out with support from the Netherlands Organisatie voor Wetenschappelijk Onderzoek and US National Science Foundation Grants AST 99-87654 and 00-98685. This work made use of the NASA ADS astronomical data system.

References

- Backer, D. C., Rankin, J. M., & Campbell, D. B. 1974, *ApJ*, 197, 481
 Bartel, N. 1981, *A&A*, 97, 384
 Bartel, N., Kardeshev, N. S., Kuzmin, A. D., et al. 1981, *A&A*, 93, 85
 Cole, T. W. 1970, *Nature*, 227, 788
 Davies, J. G., Lyne, A. G., Smith, F. G., et al. 1984, *MNRAS*, 211, 57
 Drake, F. D., & Craft, H. D. Jr 1968, *Nature*, 220, 231
 Edwards, R. T., & Stappers, B. W. 2003, *A&A*, 410, 961
 Edwards, R. T., & Stappers, B. W. 2004, *A&A*, 421, 681
 Gould, D. M., & Lyne, A. G. 1998, *MNRAS*, 301, 253
 Lyne, A. G., Smith, F. G., & Graham, D. A. 1971, *MNRAS*, 153, 337
 Manchester, R. N. 1971, *ApJS*, 23, 283
 Manchester, R. N., Taylor, J. H., & Huguenin, G. R. 1975, *ApJ*, 196, 83
 Page, C. G. 1973, *MNRAS*, 163, 29
 Ramachandran, R., Rankin, J. M., Stappers, B. W., Kouwenhoven, M. L. A., & van Leeuwen, A. G. L. 2002, *A&A*, 381, 993
 Rankin, J. M., & Ramachandran, R. 2003, *ApJ*, 195, 513
 Taylor, J. H., & Huguenin, G. R. 1971, *ApJ*, 167, 273
 Taylor, J. H., Jura, M., & Huguenin, G. R. 1969, *Nature*, 223, 797
 Taylor J. H., Huguenin, G. R., & Manchester, R. N. 1975, *ApJ*, 195, 513
 Suleymanova, S. A., Volodin, Yu. V., & Shitov, Yu. P. 1988, *Astron. Zh.* 28, 32
 Sutton, J. M., Staelin, D. H., Price, R. M., & Weimer, R. 1970, *ApJ*, 159, L89
 van Leeuwen, A. G. L., Kouwenhoven, M. L. A., Ramachandran, R., Rankin, J. M., & Stappers, B. W. 2002, *A&A*, 387, 169
 Vitkevich, V. V., & Shitov, Yu. P. 1970, *Nature*, 225, 248
 von Hoensbroech, A., & Xilouris, K. M. 1997, *A&AS*, 126, 121
 Wolszczan, A., Bartel, N., & Sieber, W. 1981, *A&A*, 100, 91